

Recent Results on Hadronic D_s and D Meson Decays from the Mark III[†]

J. Adler, Z. Bai, G.T. Blaylock, T. Bolton, J.-C. Brient, T.E. Browder, J.S. Brown, K.O. Bunnell, M. Burchell, T.H. Burnett, R.E. Cassell, D. Coffman, V. Cook, D.H. Coward, F. DeJongh, D.E. Dorfan, J. Drinkard, G.P. Dubois, G. Eigen, K.F. Einsweiler, B.I. Eisenstein, T. Freese, C. Gatto, G. Gladding, C. Grab, J. Hauser, C.A. Heusch, D.G. Hitlin, J.M. Izen, P.C. Kim, L. Köpke, J. Labs, A. Li, W.S. Lockman, U. Mallik, C.G. Matthews, A.I. Mincer, R. Mir, P.M. Mockett, B. Nemati, A. Odian, L. Parrish, R. Partridge, D. Pitman, S.A. Plaetzer, J.D. Richman, M. Roco, H.F.W. Sadrozinski, M. Scarletella, T.L. Schalk, R.H. Schindler, A. Seiden, C. Simopoulos, A.L. Spadafora, I.E. Stockdale, W. Stockhausen, W. Toki, B. Tripsas, F. Villa, M.Z. Wang, S. Wasserbaech, A. Wattenberg, A.J. Weinstein, S. Weseler, H.J. Willutzki, D. Wisinski, W.J. Wisniewski, R. Xu, Y. Zhu

The Mark III Collaboration

California Institute of Technology, Pasadena, CA 91125
University of California at Santa Cruz, Santa Cruz, CA 95064
University of Illinois at Urbana-Champaign, Urbana, IL 61801
University of Iowa, Iowa City, IA 52242
Stanford Linear Accelerator Center, Stanford, CA 94309
University of Washington, Seattle, WA 98195

Abstract

Recent results on hadronic D_s and D decays from the Mark III collaboration are presented. The absolute branching ratio $B(D_s^+ \rightarrow \phi\pi^+)$ is studied by searching for fully reconstructed $e^+e^- \rightarrow D_s^{*\pm} D_s^\mp$ events using seven hadronic decay modes of the D_s^+ . A limit of $B(D_s^+ \rightarrow \phi\pi^+) < 4.1\%$ at 90% C.L. is obtained. Evidence is presented for the decay $D_s^+ \rightarrow f_0(975)\pi^+$ which agrees with a recent experimental observation. Upper limits are set for the relative branching ratios $B(D_s^+ \rightarrow \eta\pi^+)/B(D_s^+ \rightarrow \phi\pi^+) < 2.5$ and $B(D_s^+ \rightarrow \eta'\pi^+)/B(D_s^+ \rightarrow \phi\pi^+) < 1.9$, where the η is studied in both the $\gamma\gamma$ and the $\pi^+\pi^-\pi^0$ decay modes and the η' in the $\eta\pi^+\pi^-$, $\eta \rightarrow \gamma\gamma$ decay chain. The resonant substructure of $D^0 \rightarrow K^-\pi^+\pi^-\pi^+$ and $D^+ \rightarrow \bar{K}^0\pi^+\pi^-\pi^+$ is studied. The branching ratio of $D^0 \rightarrow \bar{K}^{*0}\rho^0$ is found to be smaller than the theoretically expected whereas the decay modes $D^0 \rightarrow a_1^+ K^-$ and $D^+ \rightarrow a_1^+ \bar{K}^0$ are found to be large and account for 50% of these final states.

*Contributed to the XIV International Symposium on Lepton and Photon
Interactions, Stanford, CA., August 7-12, 1989*

[†] This work was supported in part by the U.S. Department of Energy and the U.S. National Science Foundation under contracts DE-AC03-76SF00515, DE-AC02-76ER01195, DE-AC02-87ER40318, DE-AC03-81ER40050, and DE-AM03-76SF0034.

We report a study of hadronic D_s^+ and D decays by the Mark III experiment. The D_s^+ absolute branching ratios are investigated through a search for fully exclusive events. The $f_0\pi$, $\eta\pi$, and $\eta'\pi$ decay modes of the D_s^+ are studied in inclusive analyses. Finally, the resonant substructure of two $D \rightarrow K\pi\pi\pi$ final states are measured.

The data used in the D^0 and D^+ analyses was recorded near the peak of the $\psi(3770)$ during 1982, 1983 and 1984. The total integrated luminosity was $\int Ldt = 9.3 pb^{-1}$. This corresponds to roughly 50K produced $D\bar{D}$ events. The D_s^+ data was taken at $\sqrt{s} = 4.14$ GeV in 1986 and corresponds to a total integrated luminosity of $\int Ldt = 6.3 pb^{-1}$.

The Mark III detector¹ is a large acceptance magnetic solenoidal spectrometer optimized for the SPEAR energy range. In these analyses, data from the drift chamber, time-of-flight system (TOF), and the electromagnetic calorimeter are used. The typical momentum resolution is $\sigma_p/p = \sqrt{(.015 \times p)^2 + (.015)^2}$. For the $\psi(3770)$ data set, the TOF resolution averages 175 ps, while in the $\sqrt{s} = 4.14$ GeV data, the resolution is degraded to 200 ps. The shower counter has a resolution of $\sigma(E)/E = 18\%/\sqrt{E}$ and the efficiency is 100% for $E_\gamma > 100$ MeV.

ABSOLUTE HADRONIC BRANCHING FRACTIONS OF THE D_s^+ MESON

An upper limit on the absolute branching fraction $B(D_s^+ \rightarrow \phi\pi^+)$ is determined by searching for fully reconstructed $e^+e^- \rightarrow D_s^{*\pm}D_s^\mp$ events in the data sample collected at $\sqrt{s} = 4.14$ GeV. The following D_s^+ modes are used in the analysis: $\phi\pi^+$, \bar{K}^0K^+ , $f_0(975)\pi^+$, $\bar{K}^*(892)^0K^+$, $\bar{K}^{*0}K^{*+}$, $\phi\pi^+\pi^+\pi^-$, and $\phi\pi^+\pi^0$. The twenty-eight possible final states are considered.

For a particular final state, all combinations of photons and particle identification assignments are formed. Backgrounds are reduced by requirements on the resonant substructure of the D_s^+ decay modes. Kinematic fits are employed to select combinations which are consistent with the $e^+e^- \rightarrow D_s^{*\pm}D_s^\mp \rightarrow \gamma D_s^+ D_s^-$ hypothesis. The D_s^+ and D_s^- candidates are constrained to have equal but unspecified mass $M(X)$. Double tag events would produce a signal at the D_s^+ mass in the resulting $M(X)$ distribution. For each double tag mode, a signal region in the $M(X)$ distribution is selected which contains 95% of a Monte Carlo-generated signal. No candidate signal events are observed.

An upper limit on the $D_s^+ \rightarrow \phi\pi^+$ branching fraction $B_{\phi\pi^+}$ is obtained by computing the likelihood of observing zero candidate events as a function of $B_{\phi\pi^+}$. The measured quantities used as input are: $\sigma LB_{\phi\pi^+} = 156 \pm 38^2$, $b_{\bar{K}^0 K^+} = 0.92 \pm 0.38^3$, $b_{f_0\pi^+} = 0.28 \pm 0.10^4$, $b_{\bar{K}^{*0} K^+} = 0.93 \pm 0.12^{5-8}$, $b_{\bar{K}^{*0} K^{*+}} = 2.3 \pm 1.4^7$, $b_{\phi\pi^+\pi^+\pi^-} = 0.41 \pm 0.10^{6,7,9}$ and $b_{\phi\pi^+\pi^0} = 2.4 \pm 1.1^{10}$ where $\sigma = \sigma(e^+e^- \rightarrow D_s^{*\pm} D_s^{\mp})$, L is the integrated luminosity, and $b_i = B(D_s^+ \rightarrow \text{Mode } i)/B(D_s^+ \rightarrow \phi\pi^+)$. The likelihood function $\mathcal{L}(B_{\phi\pi^+}, \sigma LB_{\phi\pi^+}, b_i)$ is constructed by using Poisson statistics for the number of observed events, and Gaussian errors (including correlations) for the measured quantities. The likelihood is set to zero if $B_{\phi\pi^+} \sum b_i > 100\%$. The marginal likelihood $\mathcal{L}(B_{\phi\pi^+})$ is computed by integrating $\mathcal{L}(B_{\phi\pi^+}, \sigma LB_{\phi\pi^+}, b_i)$ with respect to $\sigma LB_{\phi\pi^+}$ and the b_i . The upper limit B_{90} of a 90% likelihood interval is the value of B below which 90% of the integral of $\mathcal{L}(B)$ is found. The result is $B_{90} = 3.8\%$. The uncertainty in the average detection efficiency is 8%. The upper limit is therefore increased to

$$B(D_s^+ \rightarrow \phi\pi^+) < 4.1\%$$

at 90% CL. The combined mass distribution for all final states is shown in figure 1 and the marginal likelihood is shown in figure 2.

In summary, we have obtained the first model-independent limit on the absolute branching fraction for $D_s^+ \rightarrow \phi\pi^+$. Theoretical predictions for $B_{\phi\pi^+}$ are approximately 3%^{13,24,25} consistent with the upper limit presented, and with previous estimates. The experimental results imply that a large fraction of D_s^+ decays have not yet been observed.

EVIDENCE FOR $D_s^+ \rightarrow f_0(975)\pi^+$

The $D_s^+ \rightarrow f_0(975)\pi^+$ analysis proceeds as follows. Any charged track which is not a well identified kaon by TOF is assumed to be a pion. All three pion combinations which have recoil masses close to that of the D_s^* mass (2.075-2.125 GeV/ c^2) are retained. A 1-C kinematic fit of the tracks to the hypothesis $e^+e^- \rightarrow \pi^+\pi^-\pi^\pm D_s^{*\mp}$ is performed, where the three-momentum of the D_s^* is not measured. Events with a fit probability greater than 2% are retained. There is an excess of events with $\pi^+\pi^-$ invariant mass near that of the $f_0(975)$ and $\pi^+\pi^-\pi^\pm$ mass near that of the D_s^+ . The $\pi^+\pi^-$ mass distribution is shown in figure 3 where the $\pi^+\pi^-\pi^\pm$ mass is required to lie between 1.94 and 1.98 GeV/ c^2 . The $\pi^+\pi^-\pi^\pm$

mass is shown in figure 4 where the $\pi^+\pi^-$ mass is required to lie between 0.94 and 0.98 GeV/c². The background shape is obtained by requiring the $\pi^+\pi^-$ mass to lie within the sideband region (0.86 to 0.90 GeV/c²). If all events with $\pi^+\pi^-$ combinations with masses between 0.94 and 0.98 are assumed to be from the $f_0(975)$ decay, we obtain the preliminary measurement:

$$\sigma(e^+e^- \rightarrow D_s^\pm D_s^{*\mp})B(D_s \rightarrow f_0\pi^+) = (14.9 \pm 4.2 \pm 6.5) pb$$

Using our measured rate for $\sigma(e^+e^- \rightarrow D_s^\pm D_s^{*\mp})B(D_s \rightarrow \phi\pi^+)$, we obtain the preliminary result:

$$\frac{B(D_s^+ \rightarrow f_0\pi^+)}{B(D_s^+ \rightarrow \phi\pi^+)} = .58 \pm .21 \pm .28$$

For the above measurement we assumed that the entire f_0 is contained in the mass interval, .94 – .98 GeV/c². This result will increase by a factor of two if we use the 50 MeV/c² width of the $f_0(975)$ as measured in the reaction $J/\psi \rightarrow \phi f_0$ by the Mark III. Our measurement for the ratio is in agreement with the value of $.28 \pm .10 \pm .03$ obtained by E691.²⁶

SEARCH FOR $D_s^+ \rightarrow \eta\pi^+$

The decay $D_s^+ \rightarrow \eta\pi^+$ was investigated in two final states, $\eta \rightarrow \pi^+\pi^-\pi^0$ and $\eta \rightarrow \gamma\gamma$. A combined upper limit is obtained.

$$\underline{\eta \rightarrow \pi^+\pi^-\pi^0}$$

In the analysis of the $\eta \rightarrow \pi^+\pi^-\pi^0$ decay mode a 1-C kinematic fit of all $\gamma\gamma$ candidate pairs in the event is made to the π^0 mass. Pairs for which $P(\chi^2) > 0.05$ are then used in a 2-C fit to the hypothesis $e^+e^- \rightarrow D_s^{*\pm}\pi^+\pi^-\pi^0\pi^\pm$, $\pi^0 \rightarrow \gamma\gamma$, where all combinations of the three pion candidate tracks are tried. The constraints are the π^0 mass and the mass of the unobserved $D_s^{*\pm}$. After imposing $P(\chi^2) > 0.05$ for the 2-C fit, $E_\gamma^{fit} > 70$ MeV/c² for the photons from the π^0 and the requirement that the three pion mass be within $534 < M(\pi^0\pi^+\pi^-) < 564$ MeV/c², we obtain the plot shown in figure 5. The curve includes a background whose shape is determined from the $\pi^+\pi^-\pi^0\pi^\pm$ mass distribution obtained when an $\pi^+\pi^-\pi^0$ sideband is selected outside the η region. From a maximum likelihood fit

we find an excess of 16.6 ± 6.1 events in the signal region. Correcting for the reconstruction efficiency of 12.7% and for the η branching ratio, this excess corresponds to

$$\sigma \cdot B(D_s^+ \rightarrow \eta\pi^+) = 44 \pm 16 \pm 12 \text{ pb.}$$

In the second final state that is discussed, we are unable to confirm this excess.

$\eta \rightarrow \gamma\gamma$

In the $\eta \rightarrow \gamma\gamma$ analysis all pairs of candidate photons in the event are fit to the hypothesis $\eta \rightarrow \gamma\gamma$. If the $\gamma\gamma$ pair satisfies a 1-C fit with $P(\chi^2) > 0.20$, it is used in a 2-C fit to $e^+e^- \rightarrow D_s^{*\pm}\pi^\mp\eta$, $\eta \rightarrow \gamma\gamma$, where the η mass is fixed and the missing $D_s^{*\pm}$ mass is constrained but not measured. In order to reduce combinatorial background, further cuts are used; $P(\chi^2) > 0.10$ for the 2-C fit, $E_\gamma^{hi} > 0.5 \text{ GeV}/c^2$ and $E_\gamma^{lo} > 0.2 \text{ GeV}/c^2$. The resulting $\eta\pi^+$ mass distribution is shown in figure 6. There is no evidence for a D_s^+ signal. The resulting limit, adjusting for the reconstruction efficiency of 23.6%, for the $\eta \rightarrow \gamma\gamma$ branching ratio, and allowing for systematic error is:

$$\sigma \cdot B(D_s^+ \rightarrow \eta\pi^+) < 42.5 \text{ pb.} \quad (90\% \text{ C.L.})$$

Joint Upper Limit

To properly combine these results we calculate a joint likelihood as a function of the number of produced events and we conservatively set a 90% C.L. limit of $N_{ev} < 825$ produced events. When this is combined with the integrated luminosity we obtain:

$$\sigma \cdot B(D_s^+ \rightarrow \eta\pi^+) < 66 \text{ pb} \quad (90\% \text{ C.L.})$$

Using our measured $D_s^+ \rightarrow \phi\pi^+$ cross section, we obtain the preliminary result:

$$\frac{B(D_s^+ \rightarrow \eta\pi^+)}{B(D_s^+ \rightarrow \phi\pi^+)} < 2.5 \quad (90\% \text{ C.L.})$$

SEARCH FOR $D_s^+ \rightarrow \eta' \pi^+$

The $\eta' \pi^+$ analysis is performed using the decay chain, $D_s^+ \rightarrow \eta' \pi^+$, $\eta' \rightarrow \eta \pi^+ \pi^-$, $\eta \rightarrow \gamma \gamma$. Photon candidates are selected on the basis of a 1-C fit to the η mass. We then perform a 2-C fit to the hypothesis $e^+ e^- \rightarrow D_s^{*\mp} \eta \pi^+ \pi^- \pi^\pm$, $\eta \rightarrow \gamma \gamma$, where the masses of the η and the missing $D_s^{*\mp}$ are fixed. In addition, we require; $P(\chi^2) > 0.10$ for the 2-C fit, $E_\gamma^{fit} > 0.15 \text{ GeV}/c^2$, and $|m(\eta \pi^+ \pi^-) - m_{\eta'}| < .015 \text{ GeV}/c^2$. No significant signal is observed as shown in figure 7. An upper limit is obtained. Using the measured $\sigma \times B(D_s \rightarrow \phi \pi)$, we obtain a preliminary ratio of :

$$\frac{B(D_s^+ \rightarrow \eta' \pi^+)}{B(D_s^+ \rightarrow \phi \pi^+)} < 1.9 \text{ (90\% C.L.)}$$

The $\eta \pi$ results are consistent with the measurement $\frac{B(D_s^+ \rightarrow \eta \pi^+)}{B(D_s^+ \rightarrow \phi \pi^+)} \sim 3$ from the Mark II²⁷, an early preliminary result $\frac{B(D_s^+ \rightarrow \eta \pi^+)}{B(D_s^+ \rightarrow \phi \pi^+)} = 2.6 \pm 0.6 \pm 0.8$ from the Mark III²⁸, and the limit $\frac{B(D_s^+ \rightarrow \eta \pi^+)}{B(D_s^+ \rightarrow \phi \pi^+)} < 1.5$ (90% C.L.) set by the E691.¹⁰ The $\eta' \pi$ limit is, however, much lower than the ratio $\frac{B(D_s^+ \rightarrow \eta' \pi^+)}{B(D_s^+ \rightarrow \phi \pi^+)} \sim 4.8$ reported by the Mark II.²⁷ as well as the ratio $\frac{B(D_s^+ \rightarrow \eta' \pi^+)}{B(D_s^+ \rightarrow \phi \pi^+)} = 6.9 \pm 2.4 \pm 1.4$ reported by NA14'.²⁹ These results suggest that branching ratios of the $\eta \pi$ and $\eta' \pi$ decays of the D_s may be much smaller than earlier indications.

RESONANT SUBSTRUCTURE OF $D \rightarrow K \pi \pi \pi$ DECAYS

There are several $D \rightarrow K \pi \pi \pi$ channels with very large branching ratios. To obtain a complete picture of charm decays, it is important to understand the amplitudes which contribute to this final state. In this analysis, we measure the resonant substructure of $D^0 \rightarrow K^- \pi^+ \pi^+ \pi^-$ and $D^+ \rightarrow K^0 \pi^+ \pi^+ \pi^-$. Branching ratios to vector-vector and axial vector-pseudoscalar final states are obtained.

The data was collected with the Mark III detector at the SLAC $e^+ e^-$ storage ring SPEAR near the peak of the $\psi(3770)$, which decays predominantly to $D \bar{D}$. All candidate $D \rightarrow K \pi \pi \pi$ events are kinematically constrained to the D mass, with the recoil mass allowed to vary. The signal can then be identified as a peak in the recoil mass spectrum at the D

mass. With this type of constraint, all events have the same amount of phase space for the decay throughout the entire recoil mass plot. The recoil mass plots for the two channels discussed here are shown in figure 8.

The contribution of each decay mode into each final state is determined using a maximum likelihood fit. The likelihood function L is a function in the five dimensional phase space defined by the 4-momenta of the decay products of the D candidate. It consists of a signal term L_s and a background term L_b :

$$L = \frac{R_{S/B}L_S + L_B}{R_{S/B} + 1}$$

The ratio of signal to background, $R_{S/B}$, is calculated for each event as a function of recoil mass. The function L_B is determined from a fit to the sidebands of the recoil mass plot and then fixed while the total likelihood function is fit from the signal region.

For each decay chain, we include a complex amplitude which models the physical process. These amplitudes consist of a relativistic Breit-Wigner for each resonance in the decay chain, multiplied by a matrix element which depends on the spin and parity of the intermediate resonances and final decay products. These matrix elements are derived using either the Lorentz invariant amplitude formalism or the helicity formalism. L_s is a coherent sum of these amplitudes, in which the relative fractions and phases are allowed to vary. The advantage of this approach is that the amplitudes provide a complete description of the processes in the five-dimensional phase space, and all the information available in the event is used in the fit.

The results are presented in the tables below. Projections of the fit function are shown in figure 9. The fractions have been scaled so that the likelihood function is properly normalized; due to interference, they do not sum to one. In the model of BSW, the branching fractions are $B(D^0 \rightarrow \bar{K}^{*0}\rho^0) = 6.1\%$ and $B(D^0 \rightarrow K^-a_1^+) = 5.0\%$. Our result for $D^0 \rightarrow K^-a_1^+$ is consistent with the theoretical expectation whereas the rate for $D^0 \rightarrow \bar{K}^{*0}\rho^0$ is much smaller than predicted.

Table I Results for $D^0 \rightarrow K^- \pi^+ \pi^+ \pi^-$

Amplitude	Fraction	Phase	Branching Ratio ³³
4-Body Nonresonant	$.233 \pm .025 \pm .10$	$-1.01 \pm .08$	$.021 \pm .003 \pm .009$
$\bar{K}^{*0} \rho^0$ Longitudinal	$.014 \pm .009 \pm .01$	$-2.64 \pm .28$	Sum of L and T:
$\bar{K}^{*0} \rho^0$ Transverse	$.152 \pm .021 \pm .05$	$-1.22 \pm .11$	$.023 \pm .003 \pm .007$
$K^- a_1^+$	$.442 \pm .021 \pm .10$.0	$.080 \pm .008 \pm .019$
$\bar{K}_1(1270)^- \pi^+$	$.113 \pm .028 \pm .04$	$.44 \pm .19$	$.031 \pm .008 \pm .011$
$K_1(1400)^- \pi^+$	$.011 \pm .009 \pm .03$	$.71 \pm .43$	$< .012$
$\bar{K}^{*0} \pi^+ \pi^-$	$.091 \pm .018 \pm .04$	$-3.31 \pm .11$	$.012 \pm .003 \pm .005$
$K^- \rho^0 \pi^+$	$.088 \pm .023 \pm .04$	$-.62 \pm .09$	$.008 \pm .002 \pm .004$

Table II Results for $D^+ \rightarrow \bar{K}^{*0} \pi^+ \pi^+ \pi^-$

Amplitude	Fraction	Phase	Branching Ratio ³³
4-Body Nonresonant	$.184 \pm .052 \pm .10$	$1.37 \pm .17$	$.012 \pm .004 \pm .007$
$K^- a_1^+$	$.612 \pm .053 \pm .15$.0	$.081 \pm .020 \pm .027$
$\bar{K}_1(1270)^0 \pi^+$	$.010 \pm .013 \pm .02$	$1.30 \pm .90$	$< .011$
$\bar{K}_1(1400)^0 \pi^+$	$.163 \pm .048 \pm .08$	$.24 \pm .26$	$.024 \pm .009 \pm .013$

SUMMARY

A search for fully reconstructed $D_s D_s^*$ decays is performed and none are observed. We thus obtain the upper limit, $B(D_s^+ \rightarrow \phi \pi^+) < 4.1\%$ at 90% C.L. A search is performed for the $f_0 \pi, \eta \pi$ and $\eta' \pi$ decay modes of the D_s . We confirm the existence of the first decay mode and set upper limits on the last two decay modes. An analysis of the resonant substructure of the four-body decay $D \rightarrow K \pi \pi \pi$ is performed. We observe a large $K^- a_1^+$ rate and a small $\bar{K}^{*0} \rho^0$ rate in the $D^0 \rightarrow K^- \pi^+ \pi^- \pi^+$ channel.

We gratefully acknowledge the dedicated efforts of the SPEAR staff. One of us (C. Gatto) wishes to thank the Fondazione Angelo Della Riccia for their support. This work was supported by the Department of Energy, under contracts DE-AC03-76SF00515, DE-AC02-76ER01195, DE-AC03-81ER40050, DE-AM03-76SF00034 and by the National Science Foundation.

References

1. D. Bernstein *et al.*, Nucl. Instrum. Methods **226**, 301(1984)
2. From the Mark III measurements of $\sigma B(D_s^+ \rightarrow \phi\pi^+)$ and $\sigma B(D_s^+ \rightarrow \bar{K}^{*0}K^+)$ (Reference 3) and the world average value of $B_{\bar{K}^{*0}K^+} / B_{\phi\pi^+}$.
3. J. Adler *et al.*, SLAC preprint SLAC-PUB-4952, 1989 (unpublished).
4. J.C. Anjos *et al.*, Phys. Rev. Lett. **62**, 125 (1989).
5. H. Albrecht *et al.*, Phys. Lett. B **179**, **398** (1986).
6. J.C. Anjos *et al.*, Phys. Rev. Lett. **60**, 897 (1988).
7. S. Barlag *et al.*, CERN preprint CERN-EP/88-103, 1988 (unpublished).
8. M.P. Alvarez *et al.*, CERN preprint CERN-EP/88-148, 1988 (unpublished).
9. J.A. McKenna, Ph.D. thesis, University of Toronto, report RX-1191, 1987.
10. J.C. Anjos *et al.*, Phys. Lett. **223**, 267 (1989).
11. The D_s^+ lifetime, $4.36^{+0.38}_{-0.32} \times 10^{-13}$ s, is taken from Reference 12.
12. G.P. Yost *et al.* (Particle Data Group), Phys. Lett. **204B**, 1 (1988).
13. M. Bauer, B. Stech and M. Wirbel, Z. Phys. C **34**, 103 (1987). Revised values of $a_1 = 1.2$ and $a_2 = -0.5$ are taken from B. Stech, Heidelberg report HD-THEP-87-18, 1987 (unpublished). The prediction for $B(D^0 \rightarrow K^- a_1^+)$ is from a private communication with B. Stech.
14. B.Yu. Blok and M.A. Shifman, [Sov. J. Nucl. Phys. **45**, 135 (1987); **45**, 301 (1987); **45**, 522 (1987); **46**, 767 (1987)].
15. A. Chen *et al.*, Phys. Rev. Lett. **51**, 634 (1983).
16. G. Moneti, in *Proceedings of the XXIII International Conference on High Energy Physics*, Berkeley, 1986, edited by S. Loken (World Publishing, Singapore, 1987).
17. M. Althoff *et al.*, Phys. Lett. B **136**, 130 (1984).
18. W. Braunschweig *et al.*, Z. Phys. C **35**, 317 (1987).
19. H. Albrecht *et al.*, Phys. Lett. B **146**, 111 (1984).

20. H. Albrecht *et al.*, Phys. Lett. B **187**, 425 (1987).
21. M. Derrick *et al.*, Phys. Rev. Lett. **54**, 2568 (1985).
22. S. Abachi *et al.*, Argonne National Laboratory preprint ANL-HEP-CP-86-71, 1986 (unpublished).
23. The Particle Data Group's estimate is $B_{\phi\pi^+} = (8 \pm 5)\%$ (Reference 12).
24. The D_s^+ lifetime, $4.36^{+0.38}_{-0.32} \times 10^{-13}$ s, is taken from Reference 12.
25. B.Yu. Blok and M.A. Shifman, Yad. Fiz. **45**, 841 (1987) [Sov. J. Nucl. Phys. **45**, 522 (1987)].
26. J.C. Anjos *et al.*, Phys. Rev. Lett. **62**, 125 (1989).
27. G. Wormser *et al.*, Phys. Rev. Lett. **61**, 1057 (1988). The measured cross section at $\sqrt{s} = 29 \text{ GeV}/c^2$ was $\sigma \cdot B(D_s^+ \rightarrow \eta\pi^+) = 5.2 \pm 2.2 \text{ pb}$ and $\sigma \cdot B(D_s^+ \rightarrow \eta'\pi^+) = 8.4 \pm 3.7 \text{ pb}$
28. J. C. Brient, SLAC-PUB-4607, March 1988
29. G. Wormser, preprint LAL 89-10, May 1989
30. The transverse matrix element is proportional to $\cos \phi \sin \theta_\pi^\rho \sin \theta_K^{K^*}$, where ϕ is the angle in the D^0 frame formed between the decay planes of the K^* and the ρ , θ_π^ρ is the angle in the ρ frame between the π and the D^0 and $\theta_K^{K^*}$ is the angle in the K^* frame between the K and the D^0 ,
31. The longitudinal matrix element is proportional to $\cos \theta_\pi^\rho \cos \theta_K^{K^*}$.
32. J. Adler *et al.*, Phys. Rev. Lett. **60**, 89 (1988);
33. Branching ratios were calculated using $B(D^0 \rightarrow K^-\pi^+\pi^+\pi^-) = .091 \pm .008 \pm .008$ and $B(D^+ \rightarrow \bar{K}^0\pi^+\pi^+\pi^-) = .066 \pm .015 \pm .015$ from ref 32, and the branching ratios of the intermediate resonances to the final state being studied.

FIGURE CAPTIONS

- 1) Mass distribution for Ds events. The arrows indicate the widest signal region ($\pm 20 \text{ MeV}/c^2$) among the double-tag final states which yield entries between 1.85 and $2.05 \text{ GeV}/c^2$. The shaded histogram shows the expected signal for $B_{\phi\pi^+} = 4.1\%$.
- 2) Marginal likelihood $\mathcal{L}(B_{\phi\pi^+})$. The value $B_{\phi\pi^+} = 3.8\%$ is indicated by the arrow. The vertical scale is arbitrary.
- 3) $\pi^+\pi^-$ mass distribution for (a) data and (b) Monte Carlo events
- 4) $\pi^+\pi^-\pi^\pm$ mass distribution
- 5) $\eta\pi^+$ mass distribution, $\eta \rightarrow 3\pi$ decay mode
- 6) $\eta\pi^+$ mass distribution, $\eta \rightarrow \gamma\gamma$ decay mode
- 7) $\eta'\pi$ mass distribution, in the mode $\eta' \rightarrow \eta\pi^+\pi^-$
- 8) Recoil mass distributions of (a) $K^-\pi^+\pi^+\pi^-$ and (b) $\bar{K}^0\pi^+\pi^+\pi^-$
- 9) Projections of the fit to the $D^0 \rightarrow K^-\pi^+\pi^+\pi^-$ final state for six submasses. Plot (a) shows the $K^-\pi^-$ mass distribution which has an enhancement near threshold due to the longitudinal polarization of the a_1 . Plot (b) shows the 3π mass distribution which contains a large a_1 contribution. Plots (d) and (f) show the $(\pi^+\pi^-)_{\text{hi}}$ and the $(\pi^+\pi^-)_{\text{lo}}$ mass distributions which are the higher and lower mass $\pi^+\pi^-$ combinations. Plots (c) and (e) show the $K^-\pi^+$ mass distributions formed from the recoiling tracks not used to form the mass combinations shown in plots (d) and (f), respectively.

Figure 1

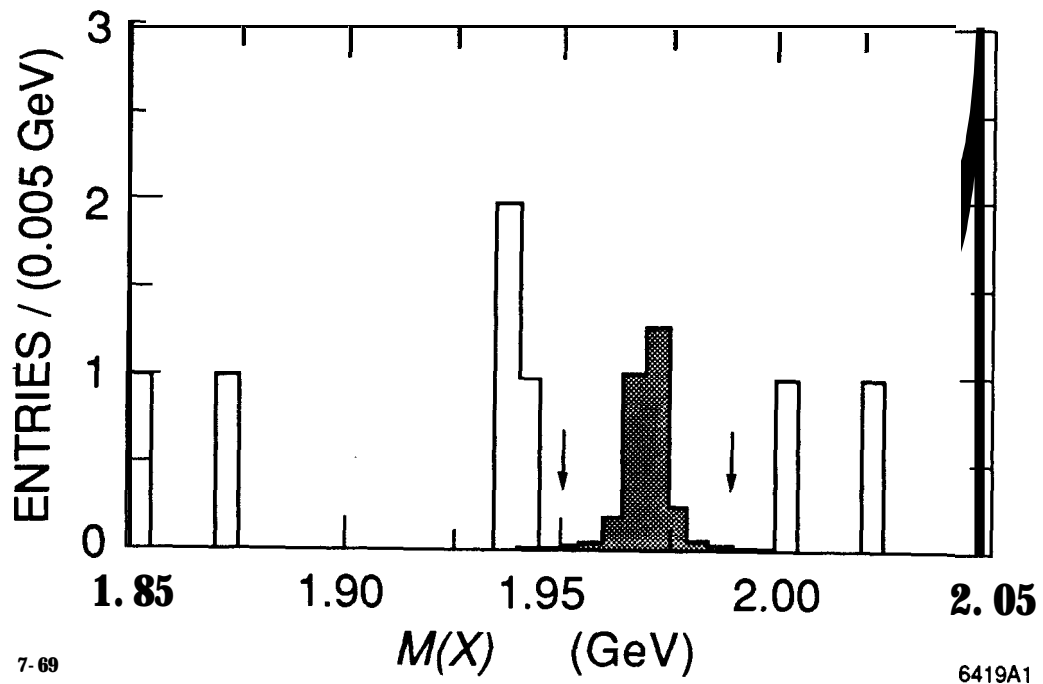


Figure 2

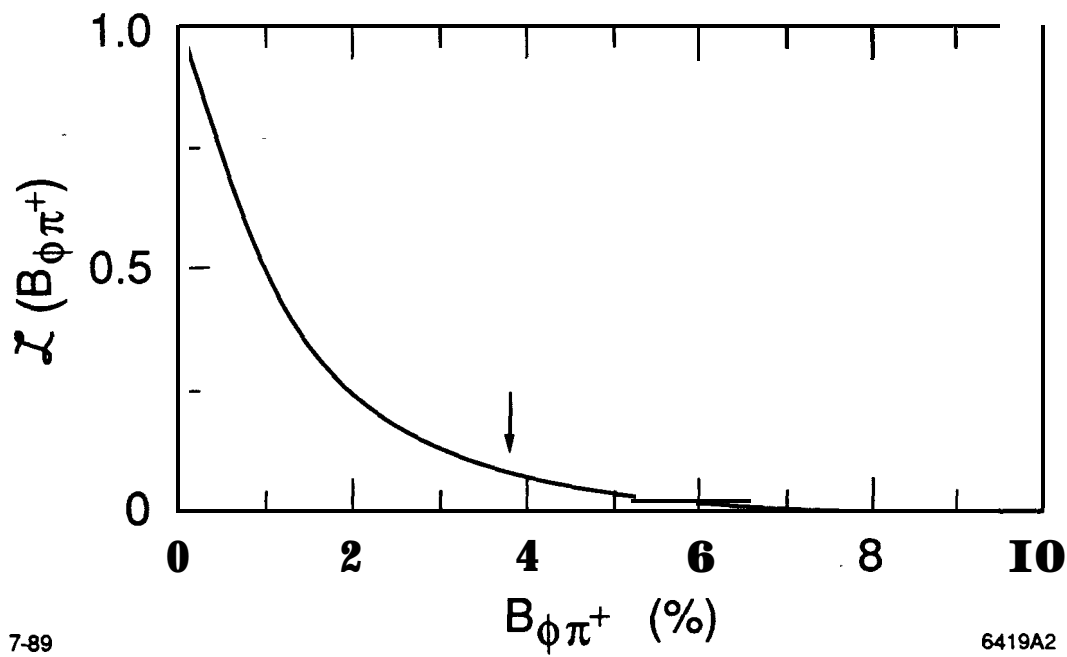


Figure 3

$\pi^+\pi^-$ mass distribution about the Ds mass

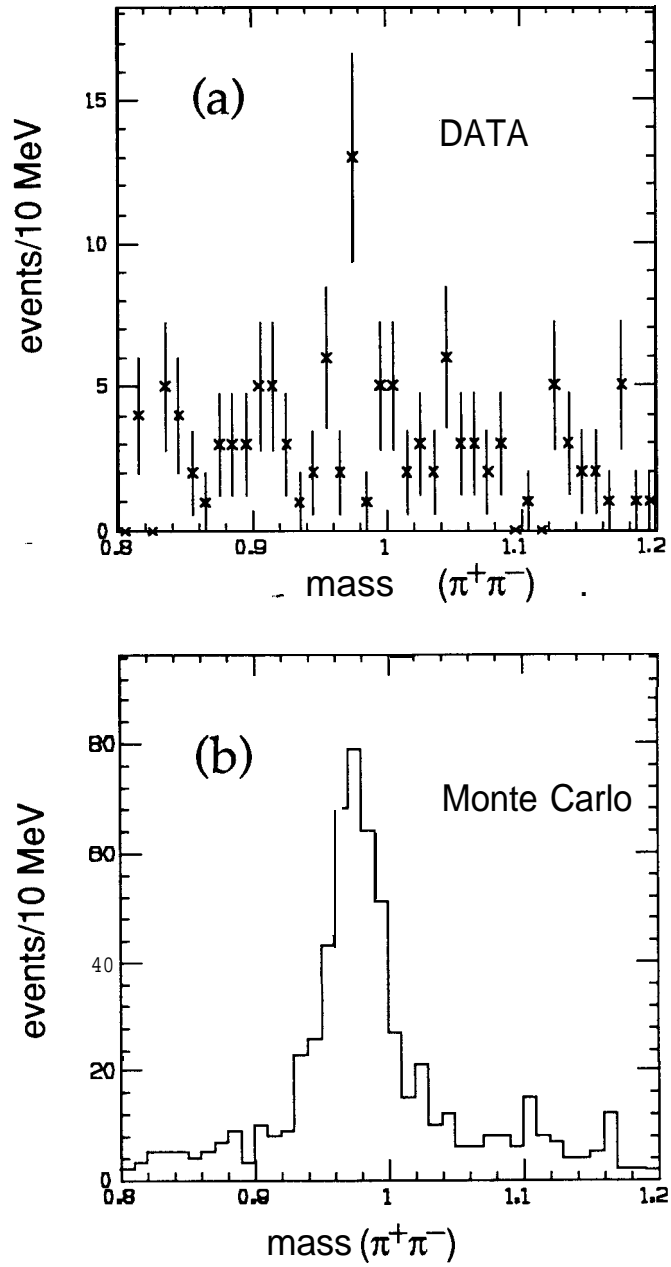


Figure 4

Fit to $\pi^+\pi^-\pi^\pm$ Mass Distribution with $D_s \rightarrow f_0\pi^+$

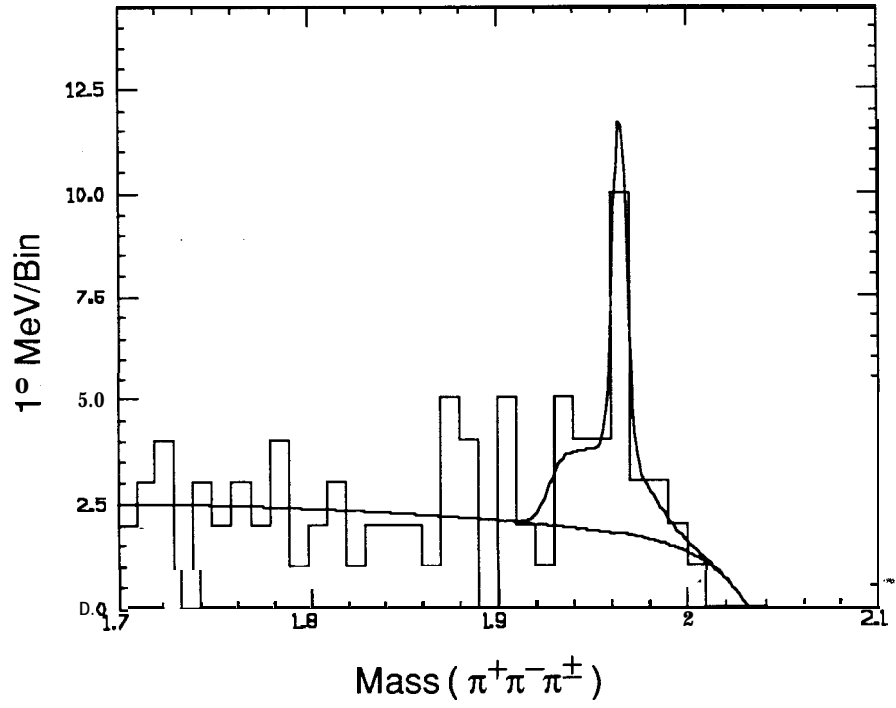


Figure 5

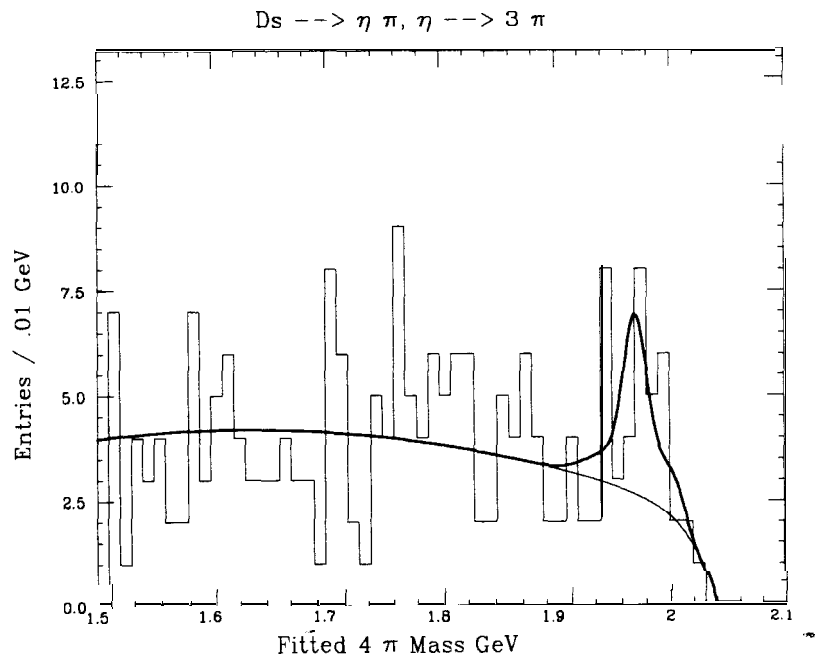


Figure 6

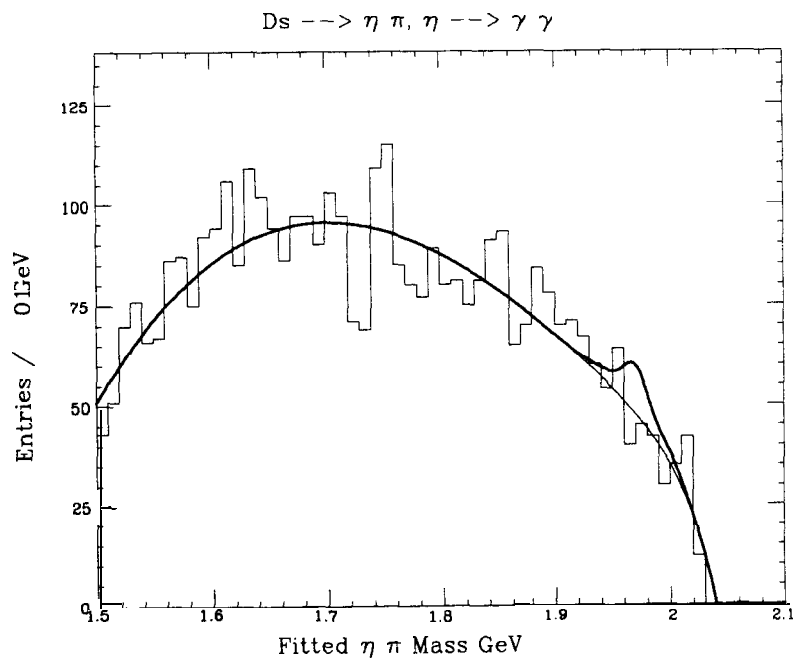


Figure 7

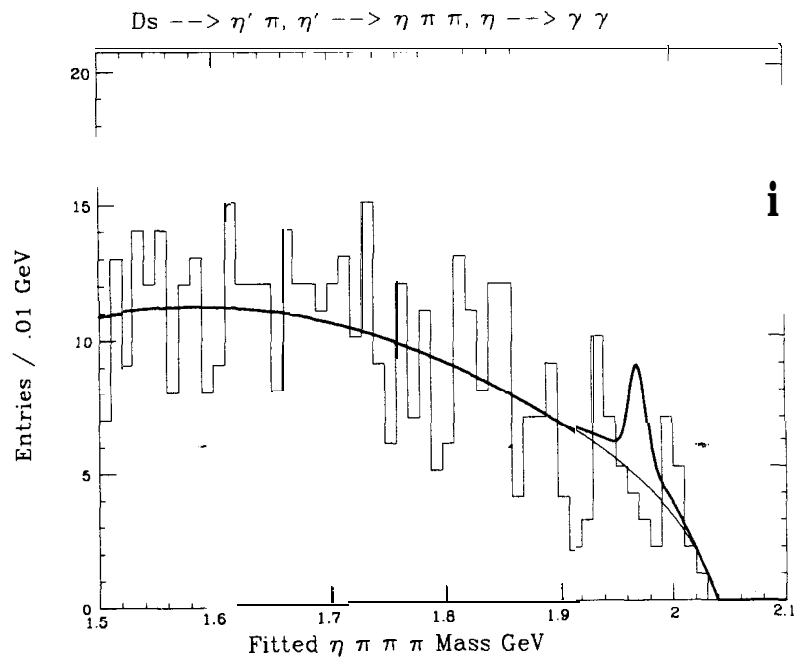


Figure 8

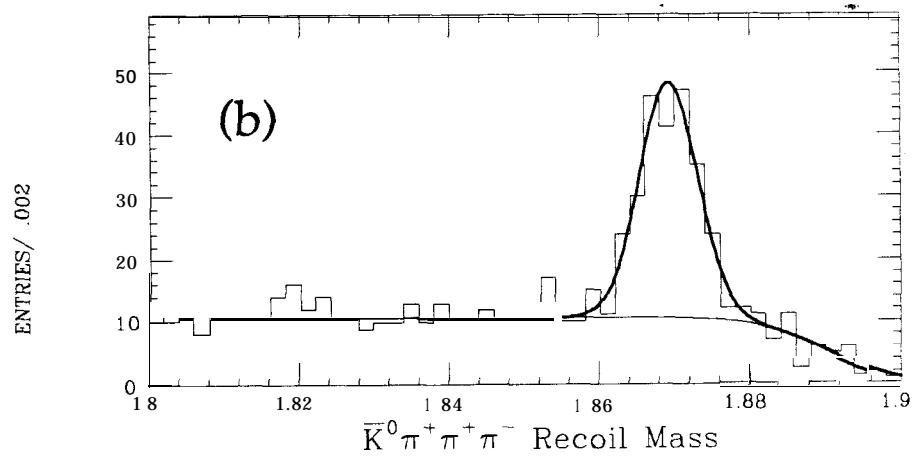
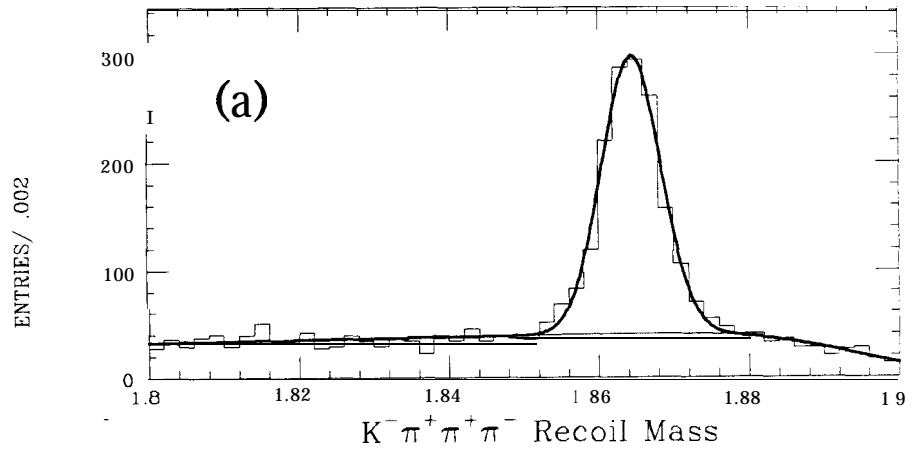


Figure 9

